0 0 0 0 4 2 5 7 9 3 0

Presented at the 4th International Conference on Sintering and Related Phenomena, Notre Dame, IN, May 25 - 27, 1975

LBL-3563
c.1

RECEIVED
LAWRENCE
BERKELEY LABORATORY

OCT 30 1975

LIBRARY AND
DOCUMENTS SECTION

THERMODYNAMIC ASPECTS OF SOLID STATE SINTERING

Joseph A. Pask and Carl E. Hoge

June 1975

Prepared for the U. S. Energy Research and Development Administration under Contract W-7405-ENG-48

For Reference

Not to be taken from this room

LAWRENCE BERKELEY LABORATORY
UNIVERSITY OF CALIFORNIA
BERKELEY

LBL-3563
c.1

DISCLAIMER

This document was prepared as an account of work sponsored by the United States Government. While this document is believed to contain correct information, neither the United States Government nor any agency thereof, nor the Regents of the University of California, nor any of their employees, makes any warranty, express or implied, or assumes any legal responsibility for the accuracy, completeness, or usefulness of any information, apparatus, product, or process disclosed, or represents that its use would not infringe privately owned rights. Reference herein to any specific commercial product, process, or service by its trade name, trademark, manufacturer, or otherwise, does not necessarily constitute or imply its endorsement, recommendation, or favoring by the United States Government or any agency thereof, or the Regents of the University of California. The views and opinions of authors expressed herein do not necessarily state or reflect those of the United States Government or any agency thereof or the Regents of the University of California.

0 0 0 0 4 2 0 7 9 6 1

THERMODYNAMIC ASPECTS OF SOLID STATE SINTERING*

Joseph A. Pask and Carl E. Hoge

Inorganic Materials Research Division, Lawrence Berkeley Laboratory and Department of Materials Science and Engineering, College of Engineering, University of California, Berkeley, California 94720

The kinetic approach, initially developed by Kuczynski,[1] based on the use of a two-sphere model has led to an understanding of the mass transport processes that can occur during solid state sintering. The factors that lead to the grain growth that are practically always observed during sintering, however, are not as well understood. The following phenomenological analysis based on a thermodynamic approach provides additional understanding of the densification processes, driving forces for mass transport, and the conditions under which grain boundary movement and consequently grain growth occur.

Because of the complexity of real systems, model systems are used to develop concepts and principles that play a role in sintering. The particles are considered to be single crystals and at chemical equilibrium. The thermodynamic analysis thus deals with interfacial energies and area changes, and is first applied to a two-sphere model and then a many-sphere model.

TWO-SPHERE MODEL

The particles are assumed to be spherical, of uniform size and with isotropic interfacial energies. On sintering, a thermodynamic driving force is realized because of the decrease in free energy due to the reduction of the surface area for the system, but the formation and growth of the grain boundary or s/s interface which is a positive contribution to the free energy of the system should also be considered. As long as δG in Eq. 1 is negative, sintering

$$\delta G = \delta\int\gamma_{sv}dA_{sv} + \delta\int\gamma_{ss}dA_{ss} \qquad (1)$$

*This work supported by the U.S. Energy Research and Development Administration.

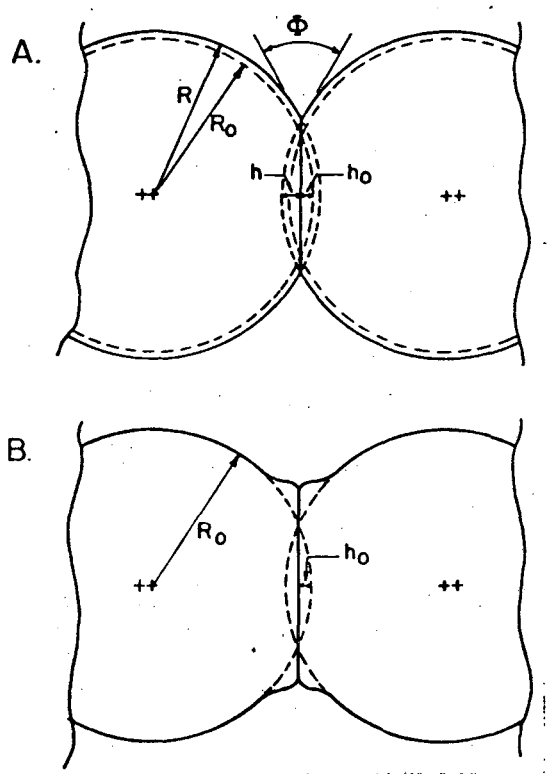

XBL 755-6351

Fig. 1. Interpenetration at two sphere contact and distribution of mass in (a) minimum free energy configuration and (b) neck region.

continues; when δG is zero, the system is at equilibrium.

Figure 1 shows ideal two-sphere models (a) without and (b) with a neck. Shrinkage is realized because of mass transport from the grain boundary to the free surfaces. In the first case the material distribution over the free surfaces is faster than the mass transport to the neck region resulting in the lowest surface area for the system at every instant. It can be shown[2] that if the system is at thermodynamic equilibrium at any point in densification, i.e. when $\delta G = 0$ according to Eq. 1, the areas can be determined and the γ_{ss}/γ_{sv} ratio calculated. This ratio also corresponds to that calculated from the dihedral angle according to Eq. 2. The fractional linear shrinkage in this case

$$\gamma_{ss}/\gamma_{sv} = 2 \cos \Phi/2 \qquad (2)$$

is equivalent to h_o/R_o, as seen in Fig. 1

In the second case the mass transport from the grain boundary to the neck region is faster than its movement from the dihedral angle region resulting in the classical neck region. With single crystal spheres a grain boundary is present which forms an equilibrium dihedral angle with the free surfaces. The surface area, however, is not at a minimum and the reverse curvature provides a

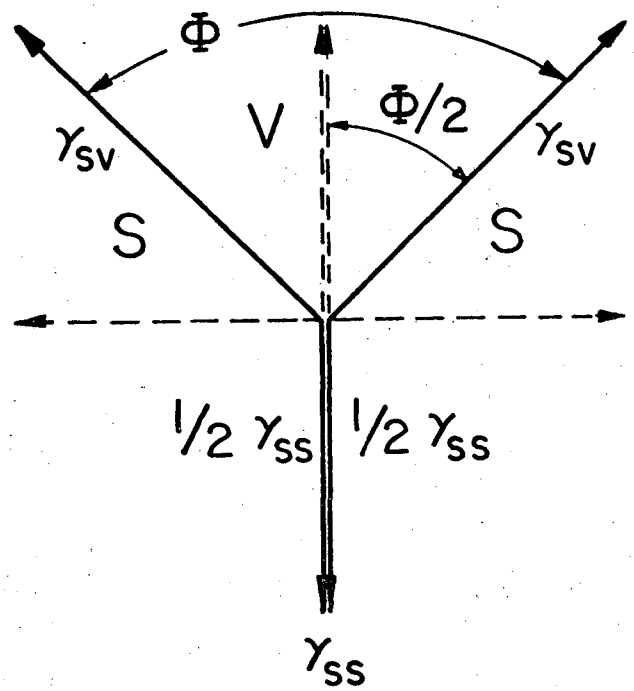

Isotropic Interfacial Energies

XBL 755-6352

Fig. 2. Solid/vapor/solid dihedral angle showing sources of tensile stresses at the grain boundary due to the components of the surface tensions perpendicular and parallel to the grain boundary.

driving force for mass transport.(3) The resulting non-equilibrium perturbations imposed on the dihedral angle are counteracted by diffusion from the grain boundary, thus effectively maintaining an equilibrium dihedral angle until the equilibrium geometric configuration of the first case is attained.

In both cases, with the stated conditions, the grain boundary grows but is not able to move because any movement would cause an increase in its area without any compensating negative free energy contribution which is energetically unfavorable.

From a geometric viewpoint, using the conditions of case (a) the sphere centers move toward each other with an experimental dihedral angle starting at zero and increasing until the equilibrium angle is reached as determined by the γ_{ss}/γ_{sv} ratio for the system. There thus exists a driving force for the angle to move to its equilibrium value.(4) Figure 2 shows the balance of forces schematically; it emphasizes the fact that for a given grain the vertical component of its surface tension is balanced by its interfacial tension in contact with the adjoining grain, e.g. energetically it favors a grain contact in preference to vapor. The

sum of the interfacial tensions for the two adjoining grains constitutes the normal grain boundary energy.

MANY-SPHERE MODEL

The same ideal conditions as before are assumed. Analyses have been carried out for simple cubic (SC), face-centered cubic (FCC), body-centered cubic (BCC), and diamond cubic (DC) packings of uniform size spheres.[2] Only one packing, SC, is discussed here to emphasize the significant points.

Figure 3(a) illustrates schematically the packing along (100) and (110) faces. For a given sphere, shrinkage occurs equally at all six contact points and the mass from the grain boundary regions is distributed uniformly as in Fig. 2(a) in order to maintain at every instant the lowest free energy for the system and to realize the relationship between interfacial areas and γ_{ss}/γ_{sv} for the system as stated in Eq. 1; during this process the experimental dihedral angle increases from 0° and the γ_{ss}/γ_{sv} ratio decreases from 2.0. When the angle reaches 90°, the (100) faces have densified (as seen in Fig. 3(b)); a closed pore exists in the center of each cube as seen along the (110) face and it is a terminal point for grain boundaries. At this stage the porosity is 3.6% and the linear shrinkage is 18.4%. Complete densification results in a linear shrinkage of 19.6% and a geometrically determined maximum dihedral angle of 109°.

Several points should be emphasized. The mass transport mechanisms are the same at every contact point and similar to that for the two-sphere model until closed pores form. Mass transport is not symmetrical in the last stage since material has to move out of the densified (100) faces in order to maintain uniform three-dimensional shrinkage. Also, the grain boundaries are energetically pinned and cannot move during the open pore period. Any perturbations on the 90° S/S/S dihedral angles that form at this point would cause grain boundary motion and grain growth since 120° S/S/S dihedral angles are at the lowest energy state.

Another significant point is that the dihedral angle of 109° and a γ_{ss}/γ_{sv} ratio of 1.416 become the critical values for this packing. If the ratio for a real system is less than 1.416, then the system has no thermodynamic barriers to reach theoretical density. On the other hand, if the real system ratio is greater than 1.416, then there will be a thermodynamic end point density.

Data for SC and the other packings are listed in Table 1. Open pores are maintained and grain boundaries cannot move up to theoretical densities of 91.2 to 96.5% depending on the type of packing. Linear shrinkage vs experimental γ_{ss}/γ_{sv} ratios are

0 0 0 0 4 2 0 7 9 6 3

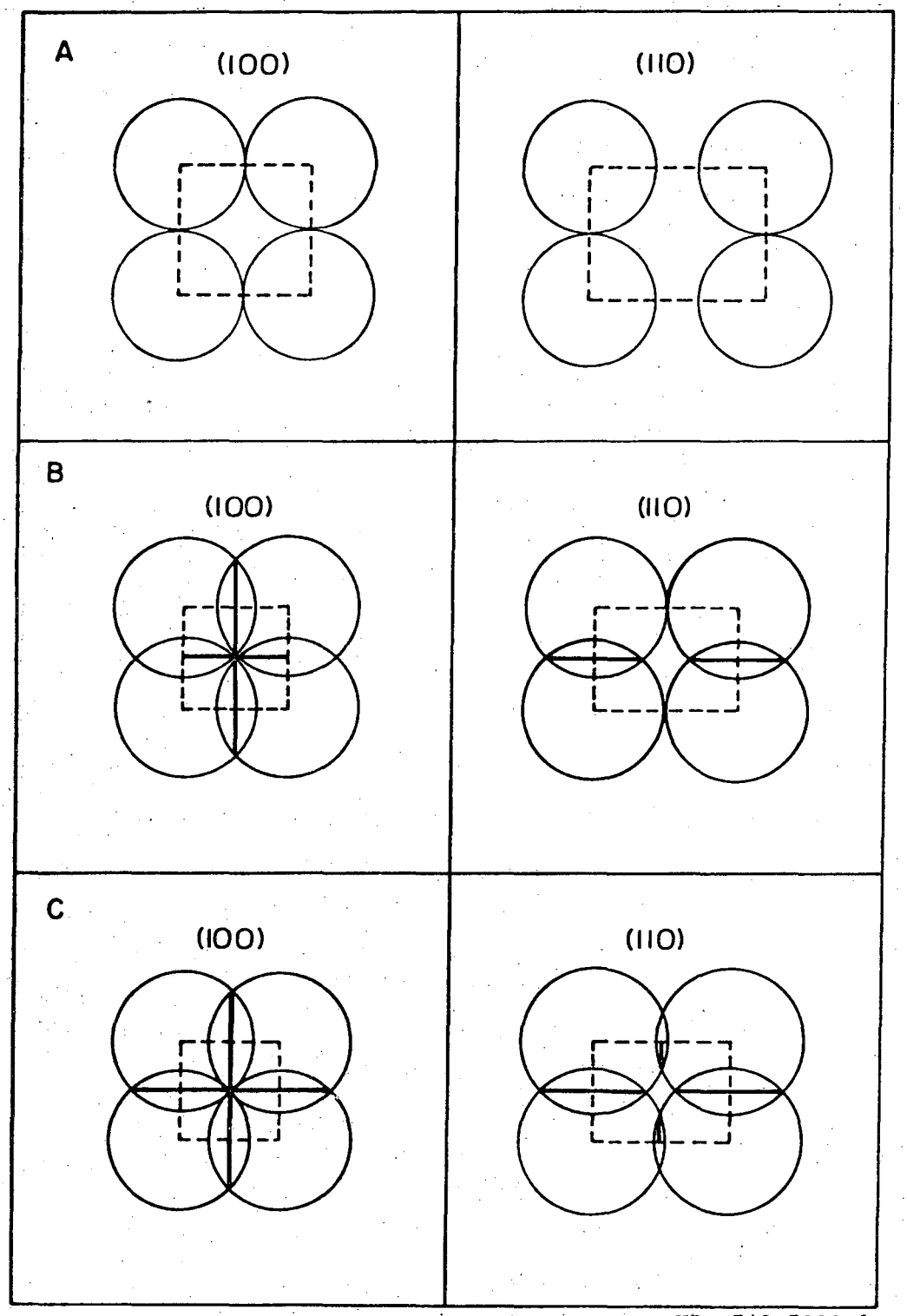

XBL 749-7293

Fig. 3. Densification steps on sintering spheres in simple cubic packing: (a) at start, (b) complete densification on (100) face, and (c) continued densification along (110) face.

plotted in Fig. 4. For uniform size spheres the shrinkage in the initial stage is essentially the same for all packings; the slight deviations are due to the fact that as the number of contacts or coordination number increases, more material is distributed in a given time causing the radius of the spheres, R in Fig. 1, to increase proportionately. Since the sintering mechanism is the same at all points of contact, the horizontal axis in Fig. 4 could represent time with zero at the right end. The rate of shrinkage would be essentially the same for all packings in the open pore stage, but the more dense packings would reach the closed pore stage in less time.

The same analysis applies to a similar series of particles of a uniform but different size. All the relationships are the same. The scale of the time axis as discussed above, however, is dependent upon the size of the spheres: shorter for smaller particles, longer for larger particles.

Disordered packings of uniform size spheres bring in some complexities. As an example, particles in a compact with an unfired theoretical density of 60% would have a statistical range of coordination numbers depending on the particle size distribution but with an average of about 7 (as determined by inspection of Table 1). The shrinkage curve as indicated in Fig. 4 would be interpolated between that for SC (52% theoretical density) and BCC (68%); the rate of shrinkage throughout the compact would be the same at the start but the higher coordination number regions would reach the closed pore stage in shorter times creating unbalances that could lead to grain boundary motion. This situation emphasizes the importance of attaining uniformity in disordered packings, e.g., an agglomerate of lower bulk density than the continuous packing becomes a region with pores because of its inability to densify completely due to the constraint of the matrix.

The analysis of the relationship of the densification of different packings to the γ_{ss}/γ_{sv} ratio indicates that the most favorable condition for a given system is the lowest γ_{ss}/γ_{sv} ratio possible. Any additives or atmospheric conditions that reduce the γ_{ss}/γ_{sv} ratio will enhance sintering, and also make it possible for some systems to densify whose natural ratio is too high. Another factor to consider is the experimental dihedral angle. Since a driving force exists for a dihedral angle to reach its equilibrium value, any conditions that would tend to keep the dihedral angle below its equilibrium value during the densification process, as described above in the non-neck-forming model system, will increase the rate of sintering. If the dihedral angle is continuously maintained at equilibrium due to the formation of a neck, the driving force for sintering is the reverse curvature in the neck region and becomes the controlling step in the sintering process.

Table 1. Parameters for solid phase sintering models

	DC	SC	BCC	FCC
Coordination number	4	6	8	12
Fractional initial void volume:	0.68	0.48	0.32	0.26
At point of second neighbor contacts:				
Linear shrinkage, h_o/R_o	0.277	0.184	0.102	0.084
Φ (dihedral angle)	104.4	89.6	59.6	59.6
γ_{ss}/γ_{sv}	1.226	1.416	1.734	1.734
Fractional void volume	0.101	0.036	0.062	0.035
At theoretical density:				
Linear shrinkage of unit cube	0.316	0.196	0.121	0.095
Φ (dihedral angle)	109		71.5	109
γ_{ss}/γ_{sv}	1.074	1.161	1.625	1.161

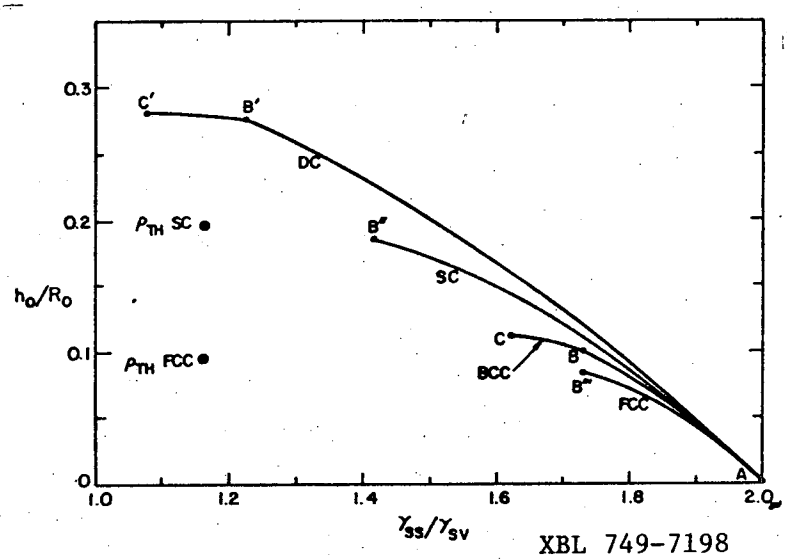

XBL 749-7198

Fig. 4. Fractional shrinkage vs critical γ_{ss}/γ_{sv} ratio for different arrays of uniform size spheres.

GRAIN BOUNDARY MOTION

In model systems as presented, grain boundaries increase in area at contact points between spheres but complete densification can occur without any grain growth in the absence of grain boundary motion. Grain growth definitely does not occur in the open pore

stage; in the closed pore stage unbalances can occur which result in grain boundary motion and grain growth. In real systems, however, it is observed that some grain growth occurs during the open pore stage. It critically affects the sintering process in the sense that growth modifies the sintering parameters and could lead to entrapment of pores within grains. Since grain growth is dependent on grain boundary motion, it is important to explore some of the factors that play a role in this process.

Anisotropy of Interfacial Energies

Appearance of flat faces, sharp edges and corner, and facets on crystals is a reflection of the existence of a significant difference in surface energies for different crystallographic faces. The particle shape favors the face that has the lowest surface energy since the free energy for the system is then at a minimum. This situation can lead to a high γ_{SS}/γ_{SV} ratio which would be detrimental to sintering.

Anisotropy also affects the dihedral angle. The S/V/S angle in Fig. 2 is symmetrical with equal γ_{SV} values and a grain boundary energy that has equal amounts of excess internal energy on either side of the S/S interface. In a symmetrical S/S/S dihedral angle the γ_{SS} values are equal and the angles are 120°. In either case if an unbalance of interfacial energies occurs at triple points, the interfaces will bend in order to realize a balance of forces and thus equilibrium angles.

Curved grain boundaries can be shown thermodynamically to have a tendency to move towards their center of curvature. A straight grain boundary, however, can also exhibit movement if the excess energies on both sides of the interface are not equal. The crystal oriented with a higher energy surface at the interface will have a driving force to grow at the expense of the other. Of, if not constrained, the orientation of the boundary can change to a lower energy state.

Movement of Grain Boundaries from Pores

Closed pores when first firmed are always associated with grain boundaries. A pore at a triple point can be shown to be pinned from energy considerations. Boundary rearrangement, however, could result in a configuration with a pore on a planar boundary.

If the boundary remains flat, it can be shown thermodynamically that the pore irregardless of the magnitude of its dihedral angle remains pinned since the energy necessary to form a continuous boundary that replaces the pore exceeds the free energy gain on spheroidization of the released pore.[2] On the other hand, if the

boundary is curved, the additional free energy gain on shortening of the boundary after breaking away makes it possible for the event to happen. It can be shown that boundaries with pores with dihedral angles up to about 73° can break away if their curvature is greater than about 26° to 36°; for pores with dihedral angles greater than about 73°, the boundaries with curvatures greater than 36° can break away.

It is possible that a boundary in a certain configuration may initially have low or no curvature, but it may curve due to anisotropy until it reaches sufficient curvature to break away from the pore. Or, it may pull a pore along leading to coalescence. It thus is apparent that any additives to a system that will tend to reduce anisotropy at the interfaces is beneficial in keeping the pores on the grain boundaries.

Range of Particle Sizes

All real particle compacts have a range of particle sizes. Two spherical particles of different sizes on sintering will form a curved boundary with its center of curvature in the direction of the smaller sphere because of the unsymmetrical dihedral angle. When the grain boundary grows to a large enough size, it will be able to move out causing the smaller grain to coalesce with the larger. This process is facilitated if a neck forms between the particles and also if the difference in particle sizes is large.

During this stage the average size of the particles is increasing, and continuous and open pores still remain. Consequently, the kinetics of sintering are also being continuously reduced. No closed pores will form in this period as long as all of the pores remain associated with grain boundaries.

It should be pointed out that the thermodynamic requirements for densification as represented by Eq. 1 are not affected by this grain growth. The δG change is associated only with the grain boundary area growth and decrease of free surface area that occur as part of the densification process. Any grain growth that occurs in densified regions is an incidental process relative to sintering.

This analysis again emphasizes the need for uniformity and homogeneity in the compact. For example, if agglomerates of lower density are dispersed in a powder that packs more densely, the powder could sinter to theoretical density and form a matrix that would restrain the agglomerates from sintering completely, resulting in an end point density for the compact. This result is not truly representative for the material since it is the result of poor processing.

CONCLUSIONS

Grain growth is extrinsic relative to sintering. Its occurrence affects sintering kinetics because of the resulting modification of sintering parameters. In an ideal system densification can occur without any grain growth, at least up to the closed pore stage.

Desirable conditions for sintering based on this analysis are:

(a) Uniform size particles as a first approximation--in any case, complete homogeneity regardless of the type of packing.

(b) Highest green density--results in less shrinkage and a larger critical γ_{ss}/γ_{sv}.

(c) As low a γ_{ss}/γ_{sv} ratio for the system as possible--achieved with additives or controlled sintering conditions.

(d) A minimum amount of anisotropy of interfacial energies--also achieved with additives or controlled sintering conditions.

(e) Experimental conditions that will tend to maintain a small experimental dihedral angle.

REFERENCES

1. George C. Kuczynski, "Self-Diffusion in Sintering of Metallic Particles," Metals Transactions of AIME, pp. 169-177, Feb. 1949.

2. Carl E. Hoge and Joseph A. Pask, "Thermodynamics of Solid State Sintering," in "Physics of Sintering, Vol. 5," edited by M. M. Ristić, Boris Kidrić, Institute of Nuclear Sciences, Beograd, Yugoslavia, pp. 109-142, Sept. 1973.

3. Conyers Herring, "Surface Tension as a Motivation for Sintering," pp. 143-179 in the Physics of Powder Metallurgy, ed. W. E. Kingston, McGraw-Hill Book Co., New York, 1951.

4. Carl E. Hoge and Joseph A. Pask, "Dihedral Angle as a Motivation for Sintering," to be published.

0 0 0 0 4 2 0 7 9 8

LEGAL NOTICE

This report was prepared as an account of work sponsored by the United States Government. Neither the United States nor the United States Energy Research and Development Administration, nor any of their employees, nor any of their contractors, subcontractors, or their employees, makes any warranty, express or implied, or assumes any legal liability or responsibility for the accuracy, completeness or usefulness of any information, apparatus, product or process disclosed, or represents that its use would not infringe privately owned rights.

TECHNICAL INFORMATION DIVISION
LAWRENCE BERKELEY LABORATORY
UNIVERSITY OF CALIFORNIA
BERKELEY, CALIFORNIA 94720